Supplementary Information for

"Quantum behavior of graphene transistors near the scaling limit"

Yanqing Wu[†*], Vasili Perebeinos[†], Yu-ming Lin, Tony Low, Fengnian Xia and Phaedon Avouris[*]

IBM Thomas J. Watson Research Center, Yorktown Heights, NY 10598

I. Metal-induced graphene heterojunctions

In a graphene p-n junction, the width of the generated barrier controls the transmission through the heterojunction. For the description of the electrostatic potential we use a model motivated by the asymptotic form of the carrier density decay away from the metal contact in the large oxide thickness limit, see Ref. [1]. Such that, the carrier density at the metal-graphene junction is given by: $n(x) = n_M l_M (1 - V_{ch}/V_M)/(x + x_B) + n_{ch}$, where n_M (V_M) and n_{ch} (V_{ch}) are the carrier density (Fermi-level) under the metal and in the graphene channel far away from the metal, respectively. The transition length is given by $l_M = 4\kappa\varepsilon_0\hbar v_F / \left(\sqrt{\pi n_M}\, e^2\right)$, where the κ is the dielectric constant controlling the width of the barrier. The value of x_B is found using the density continuity condition: $n(x=0)=n_M$. Note, that x_B coincides with the p-n junction barrier width, defined here as the distance at which the carrier density changes by half $n(x = x_B) = (n_M + n_{ch})/2$. As the carrier density in the channel is reduced by $|V_G|$, the value of the barrier width x_b increases from ~0.5 nm to a maximum of ~1.6 nm in simulations of the 50 nm device presented in the main text using κ=2.5. Note that l_M is itself gate bias dependent due to the partial pinning of the Fermi level in graphene under the metal.

The choice of κ and the channel length are critical in determining the period of Fabry-Perot oscillations observed in our two-terminal devices. Simulations with different values of κ for fixed L_{ch}=52 nm in Fig. S1 clearly show that as κ increases, the period of the oscillations increases. This is mainly because the effective channel length is reduced to $L_{ch} - 2x_b$. Since the channel length can be determined from the SEM images, the barrier width can be pinpointed by matching the period of the Fabry-Perot oscillations for the particular device.

In addition to the period of the oscillations, the barrier width determines the asymmetry of the p and n branch resistance. The measurements in 50 nm device suggest that the asymmetry in resistance (at V_G=±25 V) is about a factor of two. This is five times larger than the simulated asymmetry of about 20% using an abrupt p-n-p junction. As shown in Fig. S2 to achieve a factor of two asymmetry, a barrier width of about 10 nm is needed. However, for such a high value of a barrier width the period of oscillations would be much larger than that observed in the experiment, as shown in Fig S3.

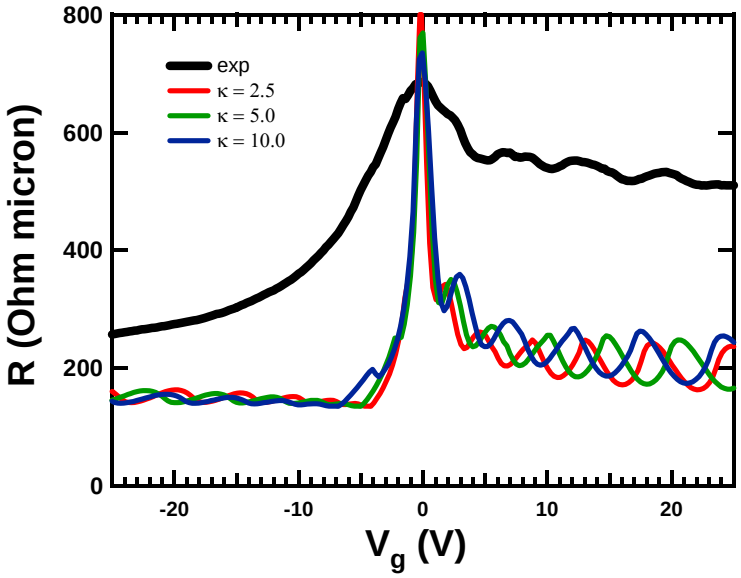

Figure S1. Oscillation period dependence on κ for κ=2.5 (red), 5.0 (green), and 10.0 (blue). As κ increases , the period of the oscillations increases accordingly. The black solid curve shows data for the 50 nm device. In the simulations we used V_0 = 100 meV, d_1=0 (fully pinned Fermi-level underneath the metal), n_{pd}=0, V_{pd}=0, L_{cav}=52 nm, T_e= 4 K.

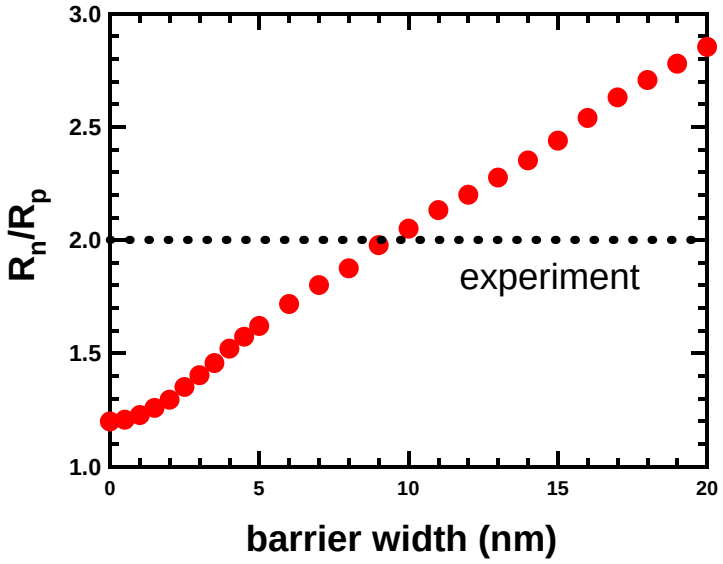

Figure S2. Resistance asymmetry simulated at V_G=±25 V using a trapezoidal potential barrier with the width being the distance where the potential is changed by a half. In the simulations (red circles), we used T_{MG}=1, V_0 = 100 meV, d_1=0 (fully pinned Fermi-level underneath the metal), n_{pd}=0, V_{pd}=0, L_{ch}=1 μm, T_e=300 K. The width of the junction barrier needed to ascribe the observed asymmetry to chiral tunneling alone is 10 nm and this conclusion is not sensitive to the shape of the junction barrier chosen[2].

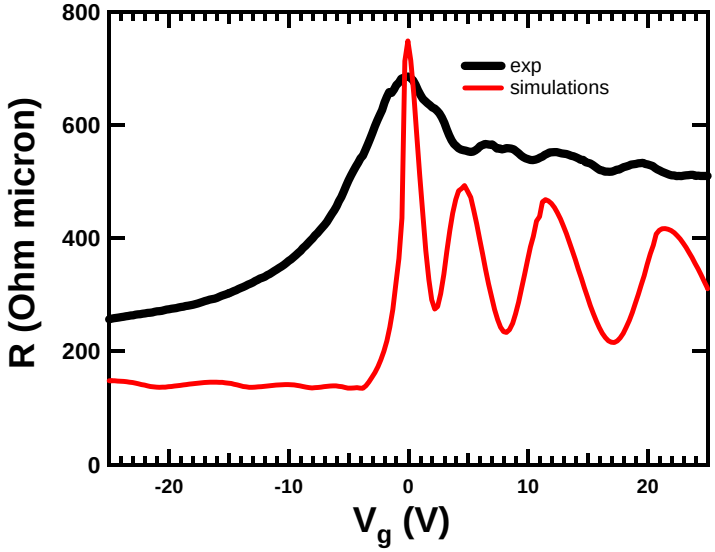

Figure S3. Fabry-Perot oscillations in the case of large junction barrier width of 10 nm. The black solid curve shows data for the 50 nm device. For the simulation (red curve), we used V_0 = 100 meV, d_1=0 (fully pinned Fermi-level underneath the metal), n_{pd}=0, V_{pd}=0, L_{cav}=52 nm, and a trapezoidal shape of the barrier. Note, there is a factor of two asymmetry between the averaged resistances on the n- and p-sides and a much larger amplitude of the oscillations due to the smaller transmission on the n-side.

II. Broadening of density of states

It is essential to use broadening to account for the experimentally observed asymmetry and maximum resistance. Electrostatic potential fluctuations lead to a variation of the charge carrier density in graphene under the metal and in the channel.

To account for the electron-hole puddles formed in the channel, we assume electron and hole rich regions with carrier densities $-\sqrt{n^2+n_{pd}^2}$ and $\sqrt{n^2+n_{pd}^2}$, respectively, distributed with probabilities given by:

$$p_{e,h}=\frac{1}{2}\left(1\pm\frac{n}{\sqrt{n^2+n_{pd}^2}}\right) \qquad (1)$$

where n_{pd} is a electron-hole puddle density and n is an averaged carrier density in the channel: $n=\langle n\rangle=p_h\sqrt{n^2+n_{pd}^2}-p_e\sqrt{n^2+n_{pd}^2}$. Note, that the second moment of distribution in Eq. (1): $\langle n^2\rangle=\int_{-\infty}^{\infty}n^2dnP(n)=n^2+n_{pd}^2$ coincides with that of a Gaussian distribution: $P_G(x)=\frac{\exp\left(-(x-n)^2/2n_{pd}^2\right)}{\sqrt{2\pi}n_{pd}}$. The distribution in Eq. (1) not only matches the first two moments of the Gaussian distribution, but it also satisfies the "sigma"-rule, i.e. the probability to find minority carrier density p_e=15% for n=n_{pd}, in agreement with a Gaussian distribution: $\int_{-\infty}^{0}dxP_G(x,n=n_{pd})=16\%$. Computationally, however, it is much more efficient to use the distribution of Eq. (1) than a Gaussian distribution.

Similarly, we model electron and hole rich regions in graphene underneath the metal with Dirac points at $\pm\sqrt{V_M^2+V_{pdM}^2}$ and probabilities to find these regions:

$$p_{e,h}=\frac{1}{2}\left(1\pm\frac{V_M}{\sqrt{V_M^2+V_{pdM}^2}}\right) \qquad (2)$$

where V_{pdM} determines the variation of the electrostatic potential underneath the metal, and the averaged electrostatic potential V_M is controlled by the metal graphene charge transfer and the back gate voltage using the same model as in Ref. [2]:

$$en_M=-C_{BG}(V_G-V_0+V_M)+C_M(V_0-V_M)=C_q e\left(eV_M\right)\left|eV_M\right|$$

where $C_M=\varepsilon_0/d_1$, $C_q=\left(\pi\hbar^2v_F^2\right)^{-1}$, and d_1 is an effective graphene metal distance.

†These authors contributed equally to this work.

*Email: avouris@us.ibm.com (P.A.) and ywu@us.ibm.com (Y.W.)

References

1. Khomyakov, P. A., Starikov, A. A., Brocks, G. & Kelly, P. J. Nonlinear screening of charges induced in graphene by metal contacts. *Phys. Rev. B* **82**, 115437 (2010).
2. Xia, F., Perebeinos, V., Lin, Y.-M., Wu, Y. & Avouris, Ph. The origins and limits of metal-graphene junction resistance. *Nature Nanotech.* **6**, 179-184 (2011).